Coexistence of bandlike and localized $5f$ electrons in $U_xLa_{1-x}S$

M. Broschwitz, C. Stellmach, M. Rode, M. Marutzky, D. Menzel, and J. Schoenes
Institut für Halbleiterphysik und Optik and Hochmagnetfeldanlage, Technische Universität Braunschweig, Mendelssohnstr. 3, D-38106 Braunschweig, Germany

O. Vogt and K. Mattenberger
Laboratorium für Festkörperphysik, ETH Zürich, Hönggerberg, CH-8093 Zürich, Switzerland
(Received 14 August 2003; revised manuscript received 21 January 2004; published 17 May 2004)

The optical and magneto-optical properties of $U_xLa_{1-x}S$ single crystals have been studied for different uranium concentrations x. The infrared optical properties reveal a rapid increase of the free-carrier effective mass even at low x, which can be assigned to an admixture of $5f$ character to the conduction band. The magneto-optical Kerr spectrum of $U_{0.8}La_{0.2}S$ can be interpreted by the interplay of an optical enhancement effect and interband contributions, which have not been observed in our former study of $U_{0.55}La_{0.45}S$, i.e., for lower U concentration. The combination of the optical and magneto-optical data leads to a picture with both localized and itinerant contributions of the $5f$ electrons of uranium. Superconducting quantum interference device magnetometry has been used to investigate magnetic ordering temperatures. Magnetic ordering has been found down to $x=0.4$ with a reduced magnetocrystalline anisotropy in the middle concentration range.

DOI: 10.1103/PhysRevB.69.184408 PACS number(s): 75.50.Cc, 75.60.Ej, 78.20.Ci, 78.20.Ls

I. INTRODUCTION

The fascinating variety of magnetic properties of many rare-earth and actinide monochalcogenides and monopnictides has motivated a large number of publications (see, for example, Ref. 1). Of special interest is the question, whether the f electrons behave more like localized or like itinerant states. Generally, the degree of f electron localization is higher for the $4f$ than for the $5f$ compounds and it increases with the atomic number within the rare-earth or actinide series.

Among these materials, uranium sulfide is known to be a strong ferromagnet with a rather bandlike character of the $5f$ electrons.[1] To reduce the overlap of neighboring U orbitals, uranium can be partly substituted by nonmagnetic ions like lanthanum or thorium. One expects an increase of f electron localization and a disappearance of ferromagnetism for highly diluted samples.

Recent investigations on the US-LaS system, however, revealed a quite complicated behavior of various physical properties as function of the amount of dilution. Schoenes *et al.*[2] found positive paramagnetic Curie temperatures for all samples with $x \geqslant 0.4$. But most strikingly, the peculiar behavior of the Pauli susceptibility and the Hall coefficient has been interpreted in terms of a two-state model, where the f electrons are partly arranged in a split-off state well below the Fermi energy and partly in a more bandlike state near E_F. Recently, such a dual nature of f electrons has been used to describe theoretically the heavy fermion system UPt_3.[3] The results of de Haas–van Alphen measurements have been reproduced properly by the assumption of such a model, which assigns the mass enhancement of the quasiparticles to the exchange interaction between the delocalized $5f$ and the localized $5f$ electrons.[3,4] In $U_xLa_{1-x}S$ magnetic phase transitions have been found by muon spin relaxation (μSR) measurements even at very low uranium concentrations.[5] In contrast, neutron-diffraction and specific-heat data exhibited a complete breakdown of long-range magnetic ordering already for $x<0.6$,[6] a result, which was supported by theory.[7] The occurrence of magnetism at lower concentrations has been assigned to short-range order in the middle concentration range.[8]

Optical investigations can be used to obtain a better insight into the electronic structure of solids. Especially the combination of optical and magneto-optical spectroscopy has been shown to be very powerful, because one can distinguish between transitions involving magnetic and nonmagnetic states.[9] A detailed analysis of the optical and magneto-optical properties of the uranium monochalcogenides and monopnictides has been used to sketch the density of states of the $5f$, $6d$, and $3p$ levels of uranium sulfide as well as the corresponding states for the other uranium monochalcogenides and monopnictides.[10,11]

Very exceptional are also the infrared properties of US. A Kramers-Kronig analysis of the reflectivity spectrum measured from 1.7 meV to 12 eV exhibited a clear structure at 40 meV, which has been assigned to a phonon-assisted optical transition.[12] Normally, phonons are not visible in the optical reflectivity of metals, because they are screened by the conduction electrons. However, in this case, the energy where the structure appears corresponds to the optical-phonon energy, and the matrix element is generated by a dipole-allowed $f \rightarrow d$ or $d \rightarrow f$ interband transition with vanishing excitation energy.[12]

In this work, we present optical measurements from the far infrared to the ultraviolet for $U_xLa_{1-x}S$ single crystals with different concentrations and some magneto-optical Kerr spectroscopy data to investigate the evolution of the f electron character as function of the uranium concentration. The determination of the infrared properties can be used to derive the effective masses of the conduction electrons. Furthermore, we have performed superconducting quantum device (SQUID) magnetization measurements. SQUID data provide the magnetic moments, phase transition temperatures, and information about the magnetocrystalline anisotropy.

II. EXPERIMENTAL DETAILS

$U_xLa_{1-x}S$ single crystals have been prepared by a mineralization method starting from a mixture of the corresponding ratios of pure US and LaS powder as described in Ref. 13. To remove oxide layers, the crystals have been cleaved or polished prior to the optical measurements.

Optical measurements between 1 and 4.3 eV have been performed with a home-built polarizer-sample-analyzer ellipsometer. In this technique the change of the state of polarization of linearly polarized light upon reflection on the sample is analyzed. Assuming a semi-infinite extension of the sample, the real and imaginary parts of the complex dielectric function $\tilde{\varepsilon}=\varepsilon_1-i\varepsilon_2$ are obtained simultaneously. The infrared optical properties (70–10 000 cm^{-1} corresponding to photon energies from 9 meV to 1.2 eV) have been determined with a commercial Fourier-transform infrared (FTIR) spectrometer (Bruker IFS 133v) through reflectivity measurements under near-normal incidence. The optical functions have been calculated from the reflectivity spectra using the Kramers-Kronig relation. All optical measurements have been done at room temperature.

For the polar magneto-optical Kerr measurements, a 90° polarization-modulation method as described elsewhere[14] has been applied. The sensitivity of this method reaches some thousandths of a degree. Using a liquid He cryostat, temperatures down to about 10 K could be reached. From the measurement of the Kerr rotation and Kerr ellipticity and the diagonal dielectric function the off-diagonal elements of the dielectric tensor have been calculated.

The sample magnetization was determined with a Quantum Design SQUID magnetometer. Hysteresis loops and the temperature dependence of the magnetization have been measured in fields up to 5 T in the temperature range from 2 to 200 K.

III. MAGNETIC PROPERTIES

Since the published magnetic data turn out to be quite controversial,[2,5,6] we have reexamined the temperature dependence of the magnetization for our present samples with different uranium concentrations in small magnetic fields of a few Oersted. An onset of magnetic ordering has been seen for all samples with $x \geqslant 0.4$. For US, the Curie temperature can be estimated to about 180 K, which agrees well with former results.[15] For decreasing x, T_C varies almost linearly with the uranium concentration, reaching about $T_C=50$ K for $x=0.4$, which is in agreement with the results of Grosse *et al.*,[5] while Bourdarot *et al.*[6] find this behavior only for $x \geqslant 0.6$.

It should be noted, that a small amount of a second magnetic phase exists for the $U_{0.4}La_{0.6}S$ sample. Such a second phase has also been found in some samples with $0.3 \leqslant x \leqslant 0.6$. Its transition temperature exceeds 150 K. Therefore, we assign this magnetic phase transition to clusters of pure uranium sulfide, which have not been dissolved during the crystal growth.

A remarkable property of US is also its large anisotropy constant of $K_1 \approx 10^8$ J m^{-3}.[16] This motivated us to investigate the evolution of the anisotropy with magnetic dilution. Figure 1 shows hysteresis loops for $U_{0.8}La_{0.2}S$ and $U_{0.55}La_{0.45}S$ at $T=10$ K along different crystallographic directions.

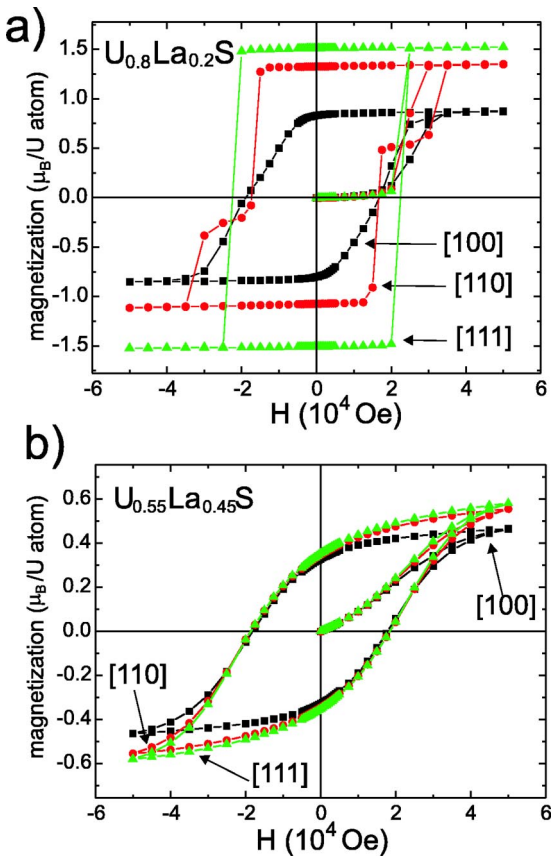

FIG. 1. (Color online) SQUID hysteresis loops of $U_{0.8}La_{0.2}S$ (a) and $U_{0.55}La_{0.45}S$ (b) in [100], [110], and [111] directions. The measurements have been performed at $T=10$ K.

In the case of $U_{0.8}La_{0.2}S$, the easy axis of the magnetization lies in the [111] direction with a coercivity of about 20 kOe. This value is much larger than the already large value found for US.[17] Saturation is reached at about 25 kOe, where the magnetic moment per uranium atom could be estimated to $1.52\mu_B$/U atom. Even in external fields of more than 50 kOe applied along [100] or [110] it is not possible to align the magnetic moments along the external field direction. For this reason, the observed values of the maximal magnetization in [110] and [100] are 1.20 and $0.85\mu_B$/U atom, respectively. The agreement with the expected values for the projection onto the [111] direction (1.24 and $0.88\mu_B$/U atom) is within the accuracy of the measurements.

In the case of $U_{0.55}La_{0.45}S$, the magnetic moment is reduced to about $0.6\mu_B$/U atom.[18] From Fig. 1(b) it can be seen that the anisotropy is strongly reduced for this uranium concentration, while the easy axis is still along the [111] direction. The shape of the hysteresis loop is different to that of the less diluted samples and exhibits a smoother change of the magnetization with the applied field. The reason for this difference could be a broad distribution of pinning centers and domains due to a reduced crystallinity in the middle concentration range. This assumption is backed up by recent

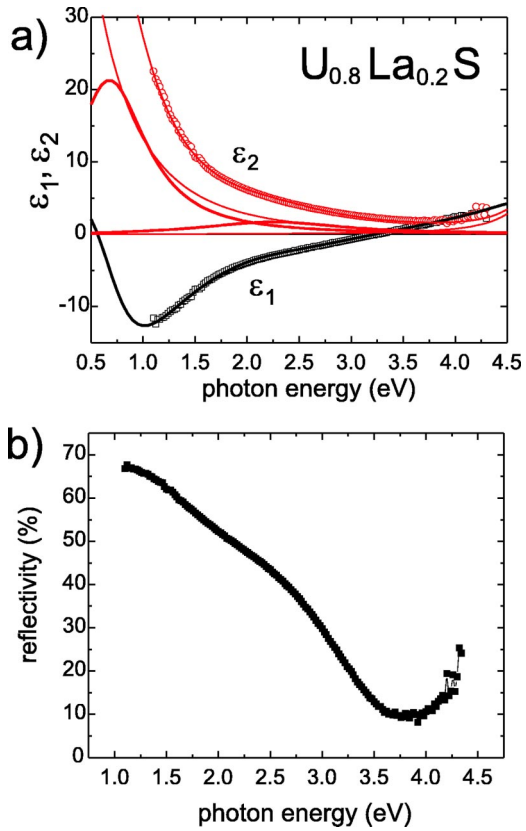

FIG. 2. (Color online) (a) Dielectric function of $U_{0.8}La_{0.2}S$. The solid lines depict a fit with the Drude-Lorentz model and a decomposition of ε_2 into single Lorentz oscillators and a Drude contribution originating from the conduction electrons. (b) Normal-incidence reflectivity calculated from ellipsometric data.

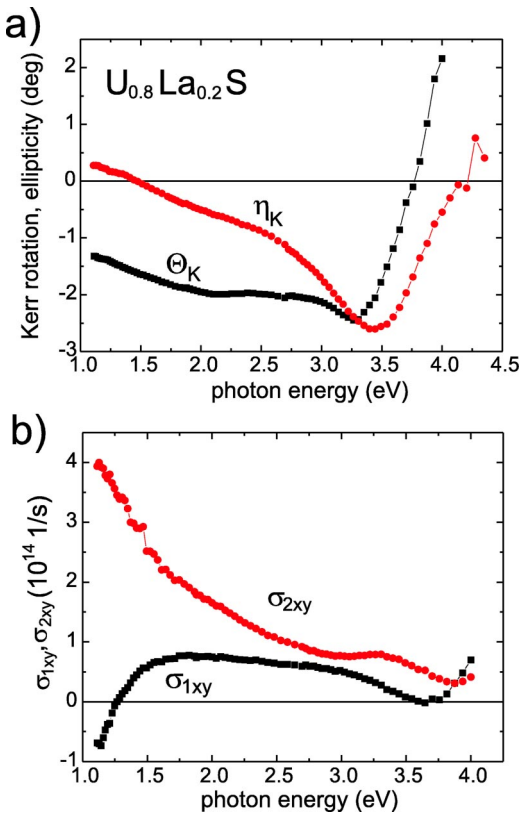

FIG. 3. (Color online) (a) Magneto-optical polar Kerr effect of $U_{0.8}La_{0.2}S$ at $T=10$ K and $B=32$ kOe. (b) Off-diagonal conductivity calculated from ellipsometric and Kerr data.

investigations of the structural properties of $U_xLa_{1-x}S$. Strong deviations from Vegard's law have been found both by neutron scattering and extended x-ray-absorption fine-structure measurements.[8,19] Even at 50 kOe, the sample is not fully saturated, but magneto-optical Kerr hysteresis loops show an only slight increase of the magnetization for higher fields.[18] For the $U_{0.4}La_{0.6}S$ sample, the hysteretic behavior is similar to that of the $U_{0.55}La_{0.45}S$ sample, but the coercivity is reduced to 12 kOe. The ordered magnetic moments obtained from the magnetization at 50 kOe exceed $0.5\mu_B$/U atom for all samples with $x \geqslant 0.4$. However, it was not possible to derive values of the anisotropy constant in dependence of x from our magnetic data.

IV. OPTICAL AND MAGNETO-OPTICAL RESULTS

A. Dielectric tensor of $U_{0.8}La_{0.2}S$

The optical and magneto-optical properties of $U_{0.55}La_{0.45}S$ have already been discussed elsewhere.[18] Therefore, Fig. 2 concentrates on the dielectric function of the cleaved $U_{0.8}La_{0.2}S$ sample as well as its normal-incidence reflectivity R calculated from the ellipsometric data. To analyze the optical data, the Lorentz-Drude model was used, which treats the bound electrons as harmonic oscillators with resonance frequencies ω_i.[9] We were able to fit the measured $\varepsilon_1(\omega)$ and $\varepsilon_2(\omega)$ spectra with a Drude term for the free carriers (i.e., $\hbar\omega_0=0$) and three Lorentz oscillators at photon energies $\hbar\omega_i$ $(i=1,2,3)=0.8$, 2.4, and 4.9 eV, respectively. From a comparison with the spectrum of pure US,[10] we can assign the oscillator at 0.8 eV to a $5f \rightarrow 6d$ transition. Also the peak at 2.4 eV, which originates from a $6d \rightarrow 5f$ transition, can be clearly resolved in the optical spectra. However, its strength is substantially reduced compared to US. This structure has not been detected in $U_{0.55}La_{0.45}S$, where a two-oscillator fit was sufficient to describe properly the optical data.[18] As already mentioned in Ref. 18, a decrease in oscillator strength of the $d \rightarrow f$ transition is typical for an enhanced 5f electron localization. The structure in the ultraviolet range marks the onset of higher-lying interband transitions and our fits are quite insensitive to the exact energy of this oscillator.

In the optical reflectivity [Fig. 2(b)], the $6d \rightarrow 5f$ transition appears as a weak shoulder. The values of R are large in the visible spectral range, which explains the metal-like appearance of the sample. The golden color of this sample is less pronounced than that of LaS or $U_xLa_{1-x}S$ bulk samples with lower uranium content, because for $x=0.8$ the plasma-edge reflectivity minimum lies in the ultraviolet spectral range at about 3.7 eV.

The magneto-optical Kerr effect, measured at $T \approx 10$ K in an external field of 32 kOe, where the magnetization stays constant, is shown in Fig. 3. The main structures in the Kerr rotation θ_K and Kerr ellipticity η_K spectra evolve at about 3.5 eV, near the optical reflectivity minimum. Although the

spectra are quite different from those for $U_{0.55}La_{0.45}S$, one can assign the minimum in η_K and the resonancelike peak in Θ_K to an optical enhancement effect like in $U_{0.55}La_{0.45}S$. The relations between the off-diagonal conductivity $\tilde{\sigma}_{xy}=\sigma_{1xy}+i\sigma_{2xy}$, which governs the magneto-optical activity, and the experimentally accessible properties are given by[20]

$$\Theta_K=\frac{1}{\omega\varepsilon_0}\frac{B\sigma_{1xy}+A\sigma_{2xy}}{A^2+B^2}, \tag{1}$$

$$\eta_K=\frac{1}{\omega\varepsilon_0}\frac{A\sigma_{1xy}-B\sigma_{2xy}}{A^2+B^2}. \tag{2}$$

Here A and B are functions of the diagonal optical constants n and k $(n-ik=\sqrt{\tilde{\varepsilon}})$ given by

$$A=n^3-3nk^2-n, \quad B=-k^3+3n^2k-k. \tag{3}$$

As can be seen in Fig. 2(a), there exists a zero crossing of ε_1 together with a small value of ε_2 near 3.5 eV. This leads to small values of the coefficients A and B and consequently to a large Kerr effect. In the lower-energy part ($\hbar\omega<3$ eV), one can see a rapid decrease of the magnitude of η_K with decreasing photon energy, whereas Θ_K stays nearly constant down to 1.5 eV. This behavior is quite similar to the situation in pure US,[20] despite the smaller absolute values for the diluted sample.

If one looks at the off-diagonal conductivity of $U_{0.8}La_{0.2}S$ [Fig. 3(b)], one sees that the absorptive part σ_{2xy} reaches 4×10^{14} s^{-1} near 1 eV. This indicates that the magneto-optical properties in the visible and near-infrared range are governed by strong interband transitions, in contrast to the $U_{0.55}La_{0.45}S$ sample, which displayed values that are ten times smaller.[18] On the other hand, there exist three important differences between the $\tilde{\sigma}_{xy}$ spectra of $U_{0.8}La_{0.2}S$ and US. First, the $5f\rightarrow6d$ transition in the infrared is shifted to lower energies for the diluted samples, thus leading to a monotonic increase of σ_{2xy} with decreasing photon energy in the limits of our measurements. In US, the maximum of σ_{2xy} lies at about 1.5 eV. This redshift on dilution can be explained by the lowering of the Fermi energy. Since every U atom in this concentration range contributes approximately one d and one f electron to the conduction band,[2] the substitution of U by La reduces the conduction-electron concentration. Secondly, the partial suppression of the $6d\rightarrow5f$ transition near 2.4 eV causes a reduction of the magnitude of σ_{2xy} in the visible spectral range. The off-diagonal conductivity of uranium sulfide exhibits a large shoulder near 3 eV, which is much smaller in the $U_{0.8}La_{0.2}S$ sample. Finally, the maximum value of σ_{2xy} is reduced by a factor of 2 compared to US, while the net magnetization is lowered only by 20% due to the dilution and the magnetic moment per uranium atom is of comparable size in US and $U_{0.8}La_{0.2}S$. Whereas in most of the uranium monochalcogenides, and monopnictides, σ_{2xy} and accordingly the total weight $\langle\sigma_{2xy}\rangle=\int_{f-d}|\sigma_{2xy}|d\omega$ scales with the net magnetization, a similar superlinear reduction of $\langle\sigma_{2xy}\rangle$ as function of the magnetization has been found in UTe.[20] Yet, UTe is the compound within the uranium monochalcogenide series, which shows several anomalies considered as strong indications for the transition to a localized $5f$ state. Among these anomalies we cite here the Kondo-like behavior of the electrical resistivity[21] and the negative value of the elastic constant c_{12}.[22] Obviously, the dilution of US by 20% is sufficient to reduce the $f-d$ hybridization at least for some part of the f electrons sufficiently in order to decrease substantially $\langle\sigma_{2xy}\rangle$. We note that the electrical resistivity of $U_{0.8}La_{0.2}S$ is still dominated by the effect of magnetic order, while for $U_{0.6}La_{0.4}S$ the Kondo-like behavior takes over.[2]

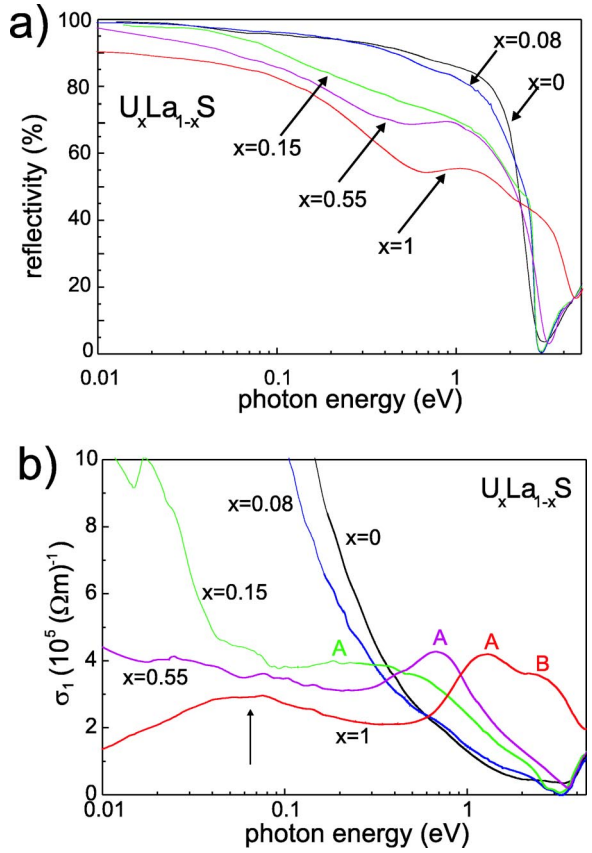

FIG. 4. (Color online) (a) Normal-incidence reflectivity of different $U_xLa_{1-x}S$ samples measured by FTIR spectroscopy and calculated from ellipsometric data (above 1.1 eV). (b) The diagonal optical conductivity σ_1 is derived from reflectivity spectra by a Kramers-Kronig analysis. The data for US have been taken from Refs. 10 and 12. Note the logarithmic energy scale in both diagrams. "*A*" and "*B*" denote the $5f\rightarrow6d$ transition and the $6d\rightarrow5f$ transition, respectively. The broad structure in US below 0.1 eV marked by the arrow has been assigned to a phonon-assisted interband transition.[12]

B. Infrared properties

Figure 4(a) shows the normal-incidence reflectivity of $U_xLa_{1-x}S$ samples with different uranium concentrations (US data taken from Refs. 10 and 12). Whereas LaS and $U_{0.08}La_{0.92}S$ show a nearly perfect Drude behavior, the reflectivity above 0.1 eV is clearly reduced for $x=0.15$ and $x=0.55$. For all compounds except US a steep plasma edge

occurs near 3 eV. A more detailed analysis can be done by Kramers-Kronig transformation of the reflectivity spectra to obtain the optical conductivity $\sigma_1 = \omega \varepsilon_0 \varepsilon_2$ [Fig. 4(b)]. The spectra of LaS and $U_{0.08}La_{0.92}S$ give no evidence for interband transitions below 3 eV.

For pure US one observes two structures, which have been assigned to $5f \rightarrow 6d(A)$ and $6d \rightarrow 5f$ transitions (B), as discussed earlier.[10] In $U_{0.55}La_{0.45}S$, structure A is still clearly visible, even if shifted to lower energies. In contrast, structure B has nearly completely vanished for $x = 0.55$. This reduction of the $d \rightarrow f$ transition indicates a stronger localization of the f electrons, as discussed quantitatively in a previous paper.[23]

Interestingly, the optical conductivity of $U_{0.15}La_{0.85}S$ deviates strongly from that of pure LaS or $U_{0.08}La_{0.92}S$. One can see a weak structure near 0.2 eV, which is possibly related to peak A occurring at higher energies for less diluted samples. Also, there are strong deviations from the Drude behavior in the spectral range below 0.2 eV. The simple Drude model does not allow a reasonable fit especially of ε_1 in the middle and far-infrared range. Therefore, the infrared properties of samples with low uranium concentration shall be discussed in the framework of the extended Drude model proposed by Allen and Mikkelsen.[24] In this model the damping parameter γ in the equation for the dielectric function of the free carriers

$$\tilde{\varepsilon}(\omega) = \frac{\omega_p^2}{-\omega^2 + i\gamma\omega} \tag{4}$$

is taken as a complex, frequency dependent quantity. This ansatz of a complex $\tilde{\gamma}(\omega)$ is needed to fulfill the causality principle for the Kramers-Kronig formalism and leads to a real frequency dependent damping and a frequency dependent effective mass m^* of the conduction electrons. The extraction of $m^*(\omega)$ and $\gamma(\omega)$ is valid for low frequencies ($\hbar\omega < 0.3$ eV in our case), where the intraband contributions dominate over the interband contributions.

Figure 5 shows the results of the fits with the extended Drude model for the frequency dependence of the effective mass (a) and the damping parameter (b). For LaS, m^* is nearly constant over the whole energy range with values slightly higher than m_0 in good agreement with former results.[25,26] The rapid increase below 0.01 eV is an artifact of the Kramers-Kronig transformation near the end of the data points. In contrast, m^* increases rapidly with decreasing photon energy for samples containing a small amount of uranium. On the other hand, γ raises strongly with photon energy in the case of $U_{0.15}La_{0.85}S$.

One can understand this change in the effective mass by the formation of a narrow, band-like $5f$ state near the Fermi level. From fits of the magnetic susceptibility with a Curie-Weiss term and a temperature dependent Pauli paramagnetism term, it was concluded that a narrow band with a Fermi energy of 0.26 eV exists in all diluted $U_xLa_{1-x}S$ compounds.[2] We identify this band with that causing the frequency dependent damping in our optical fits. Furthermore, we note that former investigations on α cerium, exhibiting also a mass enhancement in the low-energy range as well as an increase of the damping parameter with photon energy had been assigned to a partial $4f$ character of the conduction electrons.[27]

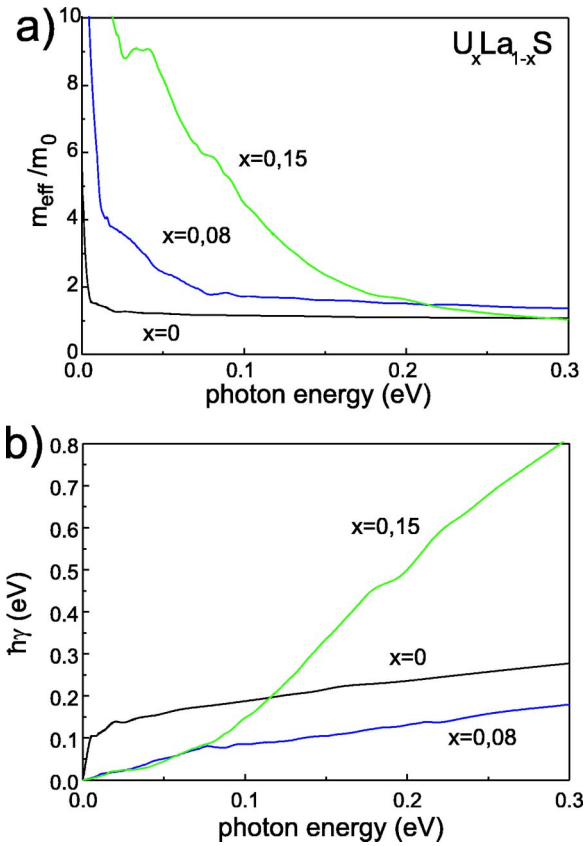

FIG. 5. (Color online) Photon energy dependence of the effective mass m^* and the damping parameter γ for $U_xLa_{1-x}S$ samples with low uranium concentrations obtained from a fit with an extended Drude model as described in Ref. 24.

V. CONCLUSION

The optical and magneto-optical investigations do not lead to a uniform picture of the $5f$ electrons. From infrared Fourier-transform spectroscopy, a substantial increase of the effective mass of the conduction electrons for low x has been found at small photon energies, pointing to the formation of a narrow conduction band with large $5f$ character at the Fermi energy. Furthermore, magneto-optical results on $U_{0.8}La_{0.2}S$ and $U_{0.55}La_{0.45}S$ (Ref. 18) indicate a stronger localized behavior of the $5f$ electrons than in US. Therefore, our analysis supports the model of the existence of two different types of f electron states in $U_xLa_{1-x}S$. The microscopic origin of this dual nature of the $5f$ electrons is not clear at present. In analogy to some Ce compounds, one might view the two states as the remainders of a bare $5f$ level and an Abrikosov-Suhl resonance. The width of 0.26 eV for the latter in the present system would, however, suggest a Kondo temperature of the order of 3000 K. This is about one order of magnitude larger than what we have de-

rived previously in the heavy fermion superconductor URu_2Si_2 from electrical resistivity measurements extending up to 1200 K (Ref. 28) and can hardly be verified by thermal measurements. Zwicknagl and Fulde,[4] on the other hand, analyzing different experimental results, start with the assumption that localized as well as itinerant $5f$ electrons are present and investigate theoretically the interplay between the hybridization of the $5f$ states with the conduction electrons and the local Coulomb correlations. For UPt_3 they find an enhancement of the effective mass of the conduction electrons by a factor of 10 over the LDA mass which agrees well with de Haas–van Alphen experiments.[4] We hope that the present results will stimulate further theoretical studies bridging the gap between the Kondo models for cerium compounds and the band models for itinerant $5f$ systems.

SQUID magnetization measurements show that magnetic ordering occurs in our $U_xLa_{1-x}S$ samples down to $x=0.4$. The large magnetocrystalline anisotropy, which has been seen for pure US is topped in $U_{0.8}La_{0.2}S$, while it is strongly reduced in the middle concentration range.

[1] O. Vogt and K. Mattenberger, in *Handbook on the Physics and Chemistry of the Rare Earths*, edited by K. Gscheidner, Jr., G.H. Lander, L. Eyring, and G. Choppin (North-Holland, Amsterdam, 1993), Vol. 17.

[2] J. Schoenes, O. Vogt, J. Löhle, F. Hulliger, and K. Mattenberger, Phys. Rev. B **53**, 14 987 (1996).

[3] G. Zwicknagl, A.N. Yaresko, and P. Fulde, Phys. Rev. B **65**, 081103 (2002).

[4] G. Zwicknagl and P. Fulde, J. Phys.: Condens. Matter **15**, S1911 (2003).

[5] G. Grosse, G.M. Kalvius, A. Kratzer, E. Schreier, F.J. Burghart, K. Mattenberger, and O. Vogt, J. Magn. Magn. Mater. **205**, 79 (1999).

[6] F. Bourdarot, A. Bombardi, P. Burlet, R. Calemczuk, G.H. Lander, F. Lapierre, J.P. Sanchez, K. Mattenberger, and O. Vogt, Eur. Phys. J. B **9**, 605 (1999).

[7] B.R. Cooper and Y.-L. Lin, J. Appl. Phys. **83**, 6432 (1998).

[8] A. Bombardi, Ph.D. thesis, University of Grenoble, 2001.

[9] J. Schoenes, in *Materials Science and Technology*, edited by W. Cahn, P. Haasen, and E.J. Kramer (VCH Verlagsgesellschaft, Weinheim, 1992), Vol. 3A, p. 147.

[10] J. Schoenes, Phys. Rep. **66**, 187 (1980).

[11] W. Reim, J. Schoenes, F. Hulliger, and O. Vogt, J. Magn. Magn. Mater. **54-57**, 1401 (1986).

[12] J. Schoenes and P. Brüesch, Solid State Commun. **38**, 151 (1981).

[13] J.C. Spirlet and O. Vogt, in *Handbook of the Physics and Chemistry of the Actinides*, edited by A.J. Freeman and G.H. Lander (North-Holland, Amsterdam, 1984).

[14] J. Metzdorf, Wiss. Ber. HMFA Braunschweig **8A** (1983).

[15] F.A. Wedgwood, J. Phys. C **5**, 2427 (1972).

[16] G.H. Lander, M.S.S. Brooks, B. Lebech, P.J. Brown, O. Vogt, and K. Mattenberger, J. Appl. Phys. **69**, 4803 (1991).

[17] D.L. Tillwick and P. de V. Du Plessis, J. Magn. Magn. Mater. **3**, 329 (1976).

[18] M. Broschwitz, J. Schoenes, M. Marutzky, O. Vogt, and K. Mattenberger, Phys. Rev. B **66**, 054425 (2002).

[19] A. Bombardi, F. d'Acapito, K. Mattenberger, O. Vogt, and G.H. Lander, Phys. Rev. B **68**, 104414 (2003).

[20] W. Reim and J. Schoenes, in *Ferromagnetic Materials*, edited by K.H.J. Buschow and E.P. Wohlfarth (Elsevier, Amsterdam, 1990), Vol. 5.

[21] B. Frick, J. Schoenes, and O. Vogt, J. Magn. Magn. Mater. **47-48**, 549 (1985).

[22] J. Neuenschwander, O. Vogt, E. Voit, and P. Wachter, Helv. Phys. Acta **58**, 781 (1985); J. Neuenschwander, H. Boppart, J. Schoenes, E. Voit, O. Vogt, and P. Wachter, in *Proceedings of the 14th Journées des Actinides, Davos*, edited by J. Schoenes (1984), p. 30.

[23] J. Schoenes and J. Alloys J. Alloys Compd. **275-277**, 148 (1998).

[24] J.W. Allen and J.C. Mikkelsen, Phys. Rev. B **15**, 2952 (1977).

[25] W. Beckenbaugh, J. Evers, G. Güntherodt, E. Kaldis, and P. Wachter, J. Phys. Chem. Solids **36**, 239 (1975).

[26] V.P. Zhuze, M.G. Karin, D.P. Lukirskii, V.M. Sergeeva, and A.I. Shelykh, Sov. Phys. Solid State **22**, 1558 (1980).

[27] J.W. van der Eb, A.B. Kuzmenko, and D. van der Marel, Phys. Rev. Lett. **86**, 3407 (2001).

[28] J. Schoenes, C. Schönenberger, J.J.M. Franse, and A.A. Menovsky, Phys. Rev. B **35**, 5375 (1987).